Environ. Sci. Technol. **1997**, *31*, 2805−2811

A Thermodynamic Approach Using Group Contribution Methods to Model the Partitioning of Semivolatile Organic Compounds on Atmospheric Particulate Matter

MYOSEON JANG, RICHARD M. KAMENS,* KERI B. LEACH, AND MICHAEL R. STROMMEN

Department of Environmental Sciences and Engineering, CB# 7400, Rosenau Hall, The University of North Carolina at Chapel Hill, Chapel Hill, North Carolina 27599-7400

Atmospheric particulate matter is a complex mixture consisting of organic and inorganic chemicals. Their sources include various combustion processes, aerosolized dusts and soils, and chemical reactions which produce secondary aerosols. The partitioning of semivolatile toxic organic compounds (SOCs) between particulate matter and the gas phase is strongly influenced by temperature, water concentration, chemical composition of the particulate matter, and the organic fraction of the particulate matter. Many investigations have recently suggested that a considerable portion of the gas−particle (G/P) partitioning in the ambient atmosphere takes place between the liquid phase of organic aerosols and the surrounding gas phase. It has been shown that the equilibrium G/P partitioning constant, K_p, of an SOC partitioning to a given particle's liquid medium is inversely related to both the activity coefficient ${}^i\gamma_{om}$ and its saturated subcooled liquid vapor pressure, p_L^o. Hence, in principal, the K_p of any SOC can be estimated from its vapor pressure and activity coefficient in a given liquid mixture. To calculate activity coefficients of SOCs in the liquid phase of different types of particles, semiempirical thermodynamic models based on additive chemical functional group methods were used. Outdoor chambers were used to generate G/P partitioning data sets for a range of SOCs in the presence of particles from wood and diesel combustion and secondary aerosols from the reaction of α-pinene with ozone. The partitioning SOCs ranged from nonpolar alkanes to polar organic acids. Plots of log (${}^i\gamma_{om}K_p$) vs log p_L^o showed a vast improvement over typical log K_p vs log p_L^o plots. These results suggest that equilibrium partitioning of many different types of SOCs can be estimated in almost any organic layer of an atmospheric aerosol.

Introduction

A simple relationship for the gas−particle partitioning of semivolatile organic compounds (SOCs) as a function of their saturated vapor pressures was observed by Bidleman *et al. (1)* and has received extensive treatment by Pankow and coworkers *(2−6)*. The original Pankow model for a homologous series of SOCs distributed between the particle and gas phases defined an equilibrium constant, K_p, at a given temperature:

$$\log K_p = \log[(F/TSP)/A] = m_r \log p_L^o + b_r \qquad (1)$$

where F is the SOC particle-phase concentration in nanograms per cubic meter, A is the gas-phase concentration in nanograms per cubic meter, TSP is the concentration of total suspended particulate matter in the atmosphere in micrograms per cubic meter, and p_L^o is the subcooled liquid vapor pressure of a semivolatile compound in millimeters of mercury. From theory *(2−6)*, the slope m_r should be close to −1 for a homologous series of compounds such as PAHs or alkanes, and b_r can be regarded as an intercept as described by Pankow *(2−6)*.

A mathematical description derived by Pankow in 1994 *(5)* for the partitioning of SOCs between the gas and the particle phases (G/P) to the outer liquid organic layer of a particle has the form of

$$K_p = (7.501RTf_{om})/(10^9 MW_{om}\,{}^i\gamma_{om} p_L^o) \qquad (2)$$

where T is temperature (K), f_{om} is the mass fraction of organic material in particulate matter, MW_{om} is the average molecular weight of a given liquid medium (g/mol), and ${}^i\gamma_{om}$ is the activity coefficient of a given organic compound, i, in a given organic mixture. When the p_L^o is in millimeters of mercury and R, the gas constant, has units of 8.31 JK^{-1} mol^{-1}, a conversion factor of 7.501 is necessary. The activity coefficient thermodynamically represents the nonideality of the SOC dissolved in the liquid layer of the particle. The activity coefficients of a given SOC vary with the composition of the organic layer associated with the particulate matter. For the purpose of this work, a new partitioning coefficient, $K_{p,\gamma}$, is defined as the product of K_p for a given compound i and its activity coefficient ${}^i\gamma_{om}$, which is a unique function of the chemical composition of the organic material in a given particle.

$$K_{p,\gamma} \equiv {}^i\gamma_{om}\, K_p \qquad (3)$$

Equation 2 in its log form becomes

$$\log K_{p,\gamma} = -\log p_L^o + \log[(7.501RTf_{om})/(10^9 MW_{om})] \qquad (4)$$

Although the equilibrium partitioning constant of organic compounds in each medium includes an activity coefficient term, linearity between log K_p and log p_L^o has been observed in the chamber studies for a homologous series of alkanes, chlorinated organics, and PAHs in ambient air *(1−7)*. This occurs because the activity coefficients for each of the compounds from a homologous series in the given aerosol mixture may often be similar. However, if one looks at compounds with different polarities and functional groups, ${}^i\gamma_{om}$ will differ from compound to compound, and a direct relationship which considers only log K_p and log p_L^o deteriorates. Combining individual log K_p values with log ${}^i\gamma_{om}$ (i.e., log $K_{p,\gamma}$) should, however, improve the relationship with log p_L^o, but this necessitates a means for estimating the activity coefficient for a given SOC in a given organic liquid mixture.

In this study, we have attempted to enhance the predictive capability for atmospheric equilibrium partitioning relationships by calculating activity coefficients using group contribution methods. The partitioning coefficients predicted from thermodynamic model approaches were compared to data obtained from outdoor smog chamber experiments. To test the utility of these approaches, different types of realistic aerosol systems *(7, 8)*, which have different polarities and liquid organic layers, were used, and a thermodynamic model

* Corresponding author e-mail: kamens@unc.edu.

TABLE 1. Conditions for the Outdoor Smog Chamber Experiments

date	particle source	chamber[a] (μg/m^3)	temp (K)	RH (%)	TSP (μg/m^3)	f_{om} (%)
Oct. 25, 1995	diesel	25 (W)	285.6	83	700	0.53
Oct. 25, 1995	wood	25 (E)	287.0	76	5070	0.98
Aug. 14, 1996	wood	25 (E)	295.2	88	3190	0.85
Aug. 5, 1996	α-pinene/O_3 reaction	190	296.3	58	1420	1.00

[a] W and E denote the designated west and east chamber.

for absorptive partitioning of SOCs on aerosols was compared to experimentally determined partitioning estimates.

Experimental Methods

Gas and particle SOC concentrations for this study were created in large outdoor Teflon film chambers *(7, 9, 10)*. All experiments were carried out in the dark. Experiments began with the addition of different types of SOCs to the gas phase of the chambers by volatilizing a "cocktail" of a liquid−solid mixture of SOCs in a hot manifold at ~200 °C *(10)*. After sampling the initial gas-phase SOCs, combustion particles were added or secondary aerosols were created in the chambers.

Wood smoke and internal combustion diesel exhaust were used as sources for combustion particles. The reaction of gas-phase α-pinene and ozone *(O_3)* was used to generate secondary aerosols. Experimental conditions are reported in Table 1. Two 25 m^3 chambers, designated as the east and west chambers, were used for the diesel exhaust and wood smoke particle experiments. A 1980 Mercedes Benz sedan (model 300SD) engine was the source of diesel emissions, and wood smoke particles were created by burning dry yellow pine in an Arrow catalytic wood stove operated in the catalytic bypass mode. To generate secondary aerosols, 0.58 ppm of ozone was added to our 190 m^3 chamber; this was followed by the volatilization of 1 mL of liquid α-pinene into the chamber atmosphere.

Gas- and particle-phase samples were simultaneously collected with a sampling train that consisted of an upstream 5-channel annular denuder, followed by a 47 mm Teflon coated glass fiber filter (type T60A20, Pallflex Products Corp., Putnam, CT), which was followed by another denuder. The detailed sampling techniques, workup procedures, and quantitative analysis have been reported in previous studies *(7−11)*. Filters for combustion particle samples were extracted in soxhlet extractors with a 40:30:30 (v/v) solvent mixture of hexane, acetone, and dichloromethane (DCM). A 50:50 hexane/DCM mixture was used to extract secondary aerosols. After extraction, filters were dried at room temperature and reweighed to estimate the mass fraction of organic particulate matter, f_{om}. Losses of filter fibers during the extraction process were addressed by extracting blank filters. This mass was typically less than 5% of the extracted mass and was applied to the calculation of f_{om}. Appreciable particulate matter was not lost in the soxhlet extracts during extraction, as evidenced by the lack of particles in the final concentrated sample volume (100 μL) which was transferred from the soxhlet receiving flasks. In addition, extraction of 0.5−1.5 mg of an aerosolized mineral dust, which has a very low organic content, showed less than a 2% difference in the filter particle mass both before and after extraction with DCM.

Quantitative analysis was carried out with a Hewlett-Packard 5890 gas chromatograph interfaced to an HP 5971A mass selective detector (MSD) using a J&W 30 m DB-5 fused silica column *(7, 10)*. Identities were referenced to authentic compounds or commercially available standards *(7)*. We have previously reported that the measurement precision in our lab through the entire workup procedure with U.S. National Institute of Standards and Technology diesel soot (SRM 1650) was generally at or below ±12.5% (±1 relative sd) for PAHs and ±15% for NPAHs *(7, 10)*.

Theory

Calculation of Activity Coefficients. The most promising method for calculating activity coefficients employs a concept called the *group contribution method*. This technique takes advantage of molecular structural information and has been used to calculate thermodynamic quantities such as molar volumes, Henry's law values, and octanol−water partitioning coefficients *(12)*. Group contribution techniques structurally subdivide compounds into functional groups. Assignments associated with these functional groups are used to calculate cohesive energies or interaction parameters, which, in turn, are used to calculate the activity coefficient of the compound *(13, 14)*. This approach has been applied to coal and crude oil systems, paint formulations and pesticides *(15)*, and biological and environmental systems *(16−19)*. Two different group contribution methods were employed in this study.

Hansen's Cohesive Energies and Solubility Parameters. Group contribution techniques for calculating activity coefficients all have the same origin; they start with the free energy of mixing, which is given in terms of its enthalpic and entropic contributions. The activity coefficient ($^i\gamma_j$) is

$$\ln {}^i\gamma_j = ({}^iV/RT)\,{}^{ij}A + {}^{ij}d \qquad (5)$$

where ^{ij}A is Hildebrand's exchange cohesive energy density, which is a quantitative measurement of the cohesive properties of a compound i in a medium j, ^iV is the molar volume of compound i, and ^{ij}d is a combinational size effect term in a binary system *(20, 21)*. A quantitative measure of the cohesive properties of a substance is the cohesive energy, E_{coh}, in joules per mole. The cohesive energy density is defined as $e_{coh} \equiv E_{coh}/{}^iV$ in joules per cubic centimeter and is closely related to the internal pressure, a quantity appearing in the equation of state. The square root of the cohesive energy density is called the solubility parameter, δ, where $\delta \equiv e_{coh}{}^{1/2}$, in (joules)$^{1/2}$ per (centimeters)$^{3/2}$, which equals $(E_{coh}/{}^iV)^{1/2}$. Solubility parameters are widely used for the correlation of chemical/solvent interactions *(22)*. The above parameters are calculated from their molar attraction constants, F_A, which are defined as $E_{coh}{}^{1/2}/{}^iV^{1/2}$. F_A values are semiempirical values for different functional groups and can be used as additive quantities. For liquids of low molecular weight, the cohesive energy, E_{coh}, is closely related to the molar heat of evaporation, ΔH_{vap}, where E_{coh} equals the internal cohesive energy, ΔU_{coh}, which equals, $\Delta H_{vap} - p\Delta V \approx \Delta H_{vap} - RT$.

In 1967, Hansen *(23)* extended Hildelbrand's original theory of the cohesive energy to polar and hydrogen-bonding systems. Hansen's original approach was developed for the solubility of solvent−polymer systems *(13)*. The group contribution parameters developed by Hansen and Beerbower *(13)* were used in the present study. It was assumed that the cohesive energy of a compound i could be divided into three parts, corresponding to the three solubility components of the interaction forces: dispersion ($^i\delta_d$), polar ($^i\delta_p$), and hydrogen bonding ($^i\delta_h$) terms, where d, p, and h denote dispersion, polar, and hydrogen bonding forces *(24−26)*:

$${}^iE_{coh} = {}^iE_d + {}^iE_p + {}^iE_h \qquad (6)$$

$${}^i\delta^2 = {}^i\delta_d{}^2 + {}^i\delta_p{}^2 + {}^i\delta_h{}^2 \qquad (7)$$

The solubility parameter, ${}^i\delta$, of compound i is then calculated by

$$ {}^i\delta = ({}^i\delta_d{}^2 + {}^i\delta_p{}^2 + {}^i\delta_h{}^2)^{1/2} \quad (8) $$

From compiled molar attraction constants, F_A, for different functional groups, it is possible to calculate the individual solubility parameter components by

$$ {}^i\delta_d = \sum F_{d,k}/{}^iV \quad (9) $$

$$ {}^i\delta_p = (\sum F^2_{p,k})^{1/2}/{}^iV \quad (10) $$

$$ {}^i\delta_h = (\sum E_{h,k}/{}^iV)^{1/2} \quad (11) $$

where k is a given functional group in an organic molecule, i.

Hildebrand's cohesive energy and Hansen's group contribution methods can be extended to a multicomponent organic mixture. The van der Waals volume of the structural units, which is bounded by the outer surface of a number of interpenetrating spheres, is approximated by the sum of the van der Waals volumes of the composing structural groups, and these are also compiled in a group contribution table *(13)*. The solubility parameters of the organic matter of a multicomponent mixture, ${}^{om}\delta$, then become

$$ {}^{om}\delta_d = \sum({}^ix \sum F_{d,k})/(\sum {}^ix\ {}^iV) \quad (12) $$

$$ {}^{om}\delta_p = [\sum({}^ix \sum F_{p,k}{}^2)]^{1/2}/(\sum {}^ix\ {}^iV) \quad (13) $$

$$ {}^{om}\delta_h = [\sum({}^ix \sum E_{h,k})/(\sum {}^ix\ {}^iV)]^{1/2} \quad (14) $$

$$ {}^i\phi = {}^ix\ {}^iV/(\sum {}^ix\ {}^iV) \quad (15) $$

$$ \sum {}^ix\ {}^iV = V_{om} \quad (16) $$

where ${}^ix$ is the mole fraction of SOC i, ${}^iV$ is the molar volume, which is also calculated from an additive rule method *(12)*, and ${}^i\phi$ is the volume fraction of a component i ($\sum {}^i\phi = 1$).

In an infinitely dilute solution, the volume fraction of organic matter, ${}^{om}\phi$, has a value of 1, and the resulting activity coefficient, ${}^i\gamma_{om}$, for a regular solution can be shown to be

$$ \ln {}^i\gamma_{om} = {}^iV[({}^{om}\delta_d - {}^i\delta_d)^2 + {}^ib({}^{om}\delta_p - {}^i\delta_p)^2 + {}^ib({}^{om}\delta_h - {}^i\delta_h)^2]/RT \quad (17) $$

where the $({}^{om}\delta - {}^i\delta)^2$ terms are measures of the interaction energies and ${}^ib$ is a weighting factor based on dispersional forces *(27)*. When the entropic effects are included, ${}^i\gamma_{om}$ in eq 17 becomes

$$ \ln {}^i\gamma_{om} = {}^iV[({}^{om}\delta_d - {}^i\delta_d)^2 + {}^ib({}^{om}\delta_p - {}^i\delta_p)^2 + {}^ib({}^{om}\delta_h - {}^i\delta_h)^2]/RT + [\ln({}^iV/V_{om}) + 1 - {}^iV/V_{om}] \quad (18) $$

The UNIFAC Model. UNIFAC, or the universal functional group activity coefficient model, is one of the commonly used thermodynamic models for predicting activity coefficients of nonelectrolytes in a liquid medium *(28, 29)*. UNIFAC has a combinational term that depends on the volume as well as the surface area of each molecule and a residual term that is fit to the experimental data. The residual term is related to the energetic group interaction parameter among different functional groups. The activity coefficient ${}^i\gamma$ is calculated from the sum of the combinational ${}^i\gamma^C$ and the residual activity coefficient ${}^i\gamma^R$ terms:

$$ \ln {}^i\gamma = \ln {}^i\gamma^C + \ln {}^i\gamma^R \quad (19) $$

The calculation procedure for the UNIFAC model has been extensively documented by many others *(13, 28−30)*. Currently we are using a FORTRAN program written by Prausnitz's group at UC-Berkeley *(31)* and a simplified mixture consisting of four to six components to approximate an aerosol liquid mixture. UNIFAC does not distinguish between isomers (e.g., phenanthrene vs anthracene and fluoranthene vs pyrene). UNIFAC also cannot compute proximity effects from intramolecular geometry. Sandler has reported various results for estimating activity coefficients using the UNIFAC model *(14)*.

Results and Discussion

Chemical Composition of Chamber Aerosols. From the above discussion, it is apparent that the chemical composition of the aerosol is of great importance in the calculation of activity coefficients. Differences in composition can be illustrated by comparing aerosols from wood and diesel combustion and secondary aerosols. Wood smoke particles contain highly polar oxygenated compounds such as substituted phenols, substituted aromatic acids, and substituted aromatic aldehydes and ketones *(32−35)*. Diesel soot, which is composed of aliphatic hydrocarbons and long-chain aliphatic acids, represents a nonpolar particle medium. Approximately 70−95% (by mass) of wood soot particles and 20−75% of diesel soot particles is extractable using organic solvents *(8, 9)*. Table 2 illustrates the compounds, mole fractions, volume fractions, and molar volumes used as inputs to the Hansen model for wood smoke and diesel combustion particles. Speciation data reported by Rogge *et al. (36, 37)* were used to create Table 2. For wood and diesel soot particles, the compounds in Table 2 represent ~20−30% of the extractable particle mass. Implicit in the use of these data is the assumption that these compounds represent the entire distribution of compounds in the organic fraction, f_{om}, of the particle. It was also assumed that all of the organic mass behaves as a liquid.

Monoterpenes are important organic compounds emitted into the troposphere from vegetation. A very important feature of monoterpene reactions is aerosol formation. The major degradation pathways of monoterpenes in the atmosphere are by reaction with ozone and by reaction with hydroxyl radicals. Hull reported that products from the reaction of α-pinene with O_3 in the gas phase included compounds such as *cis*-pinonaldehyde, *cis*-norpinonaldehyde, c*is*-pinonic acid, and norpinonic acid *(38)*. The mole fractions of the major aerosol products from the reaction of α-pinene with O_3 were constructed from Hull's work and are given in Table 3. Secondary aerosols from the α-pinene/O_3 reaction are 100% extractable in methylene chloride and consist almost entirely of organic compounds. At moderate temperatures, this aerosol behaves as a viscous liquid.

Given the constraints of the UNIFAC model, the composition of wood and diesel soot aerosols were simplified to mixtures of six components (Table 3). To calculate the water concentration in the particle organic medium, ${}^wC_{om}$, it was assumed that the water uptake by the organic layer was controlled by Henry's law and was proportional to the relative humidity, RH. The theoretical ${}^wC_{om}$ could then be estimated using the UNIFAC-calculated activity coefficient of water, ${}^w\gamma_{om}{}^\infty$, such that ${}^wC_{om} = RH/(100{}^w\gamma_{om}\ V_{om})$.

Predicted Activity Coefficients. To estimate activity coefficients by the Hansen method, it is necessary to calculate the solubility parameters, ${}^{om}\delta_d$, ${}^{om}\delta_p$, and ${}^{om}\delta_h$, for the organic phase of each of the different aerosol types. From the compositions for wood and diesel aerosols (Table 2) and for α-pinene/O_3 secondary aerosols (Table 3), estimated solubility parameters of organic media are given in Table 4. Weighting factors for given compounds (${}^ib$ values in eq 18) were taken from Ashen *et al.* (27) and listed in Table 5. Table 6 compares the resultant Hansen and UNIFAC activity coefficients for

TABLE 2. Model Chemical Compositions of Diesel Soot and Wood Smoke Particles based on Rogge *et al. (36, 37)*

compound	MW	$^{i}x^{a}$ (×100)	$^{i}V^{b}$	$^{i}\phi^{c}$ (×100)
Diesel Soot				
nonadecane	268	10.06	340.7	11.67
eicosane	282	17.80	356.8	21.62
heneicosane	296	11.51	372.9	14.61
docosane	310	5.94	389.0	7.86
tricosane	324	3.77	405.1	5.20
tetracosane	338	3.24	421.2	4.64
pentacosane	352	4.81	437.3	7.16
hexacosane	366	2.26	453.4	3.48
hexanoic acid	116	6.95	125.9	3.00
heptanoic acid	130	3.87	142.5	1.88
octanoic acid	144	2.23	159.1	1.21
nonanoic acid	158	4.71	175.7	2.82
decanoic acid	172	2.28	192.3	1.49
undecanoic acid	186	7.35	208.9	5.22
dodecanoic acid	200	1.81	225.5	1.39
hexadecanoic acid	256	3.03	287.4	2.96
octadecanoic acid	284	1.29	318.9	1.40
benzoic acid	122	7.09	100.0	2.41
total		100		100
Wood Smoke Particles				
hexadecanoic acid	258	1.29	287.4	2.59
eicosanoic acid	314	0.49	351.8	1.21
docosanoic acid	342	0.56	384.0	1.50
tetracosanoic acid	370	0.64	416.1	1.86
propanedionic acid	104	8.75	73.1	4.51
pentanedionic acid	132	1.20	105.3	0.89
dehydroabietic acid	300	2.96	263.2	5.47
sandarocopimaric acid (with Isomer)	302	6.14	273.8	11.80
3,4-dimethoxybenzoic acid	182	8.52	134.8	8.06
homovanillic acid	182	10.85	127.6	9.72
1,4-benzenediol	110	13.40	86.4	8.12
3-methyl-1,2-benzenediol	124	6.72	93.7	4.41
4-methyl-1,2-benzenediol	124	3.76	93.7	2.47
4-propyl-benzenediol	152	2.94	126.9	2.62
1-guaiacylpropane	166	2.81	149.4	2.94
2-methoxy-5-(1-propyl)-phenol	166	1.16	140.4	1.14
varatrylacetone	180	1.38	149.2	1.44
1-(2,4-dimethoxyphenyl)propane-2-one	194	1.10	165.8	1.28
guaiacylacetone	166	5.21	126.7	4.63
1-(4-hydroxy-3-methoxyphenyl)propan-2-one	180	5.21	143.8	5.24
1,4-dimethoxy-2-methylbenzene	152	4.41	138.7	4.29
vanillin	152	4.59	106.8	3.44
3,4-dimethoxybenzaldehyde	166	3.25	129.3	2.95
sitosterol	414	2.62	402.9	7.41
total		100		100

[a] Mole fraction. [b] Molar volume (cm^3/mol). [c] volume fraction.

TABLE 3. Simplified Particle Compositions for UNIFAC Calculations

diesel soot composition	^{i}x	wood smoke particle composition	^{i}x	α-pinene/O_3 aerosol composition	^{i}x
heneicosane	0.45	hexadecanoic acid	0.19	*cis*-pinonic acid	0.53
tetracosane	0.14	pentanedioic acid	0.07	norpinonic acid	0.11
hexanoic acid	0.11	homovanillic acid	0.18	*cis*-pinonaldehyde	0.23
undecanoic acid	0.17	4-propylbenzenediol	0.28	*cis*-norpinonaldehyde	0.13
hexadecanoic acid	0.06	1-guaiacylpropane	0.17		
benzoic acid	0.07	veratraldehyde	0.11		

TABLE 4. Solubility Parameters for Different Particle Liquid Media

	$^{om}\delta_d$ ($mPa^{1/2}$)	$^{om}\delta_p$ ($mPa^{1/2}$)	$^{om}\delta_h$ ($mPa^{1/2}$)	$^{om}\delta$ ($mPa^{1/2}$)	V_{om} (cm^3/mol)
α-pinene/O_3 products	18.6	7.1	10.4	22.5	139
wood smoke particle	19	5.2	13.8	24	142.5
diesel soot	16.2	0.9	4	16.7	293.9

wood smoke particles, diesel soot, and α-pinene/O_3 aerosols. We found good agreement between the two approaches for wood soot particles. Smaller activity coefficients are associated with a higher preference for the liquid particle phase. For wood smoke particles and α-pinene aerosols, the preference for partitioning into the organic phase goes from polar to nonpolar compounds: phenols > substituted aromatics with an aldehyde and long-chain alkanoic acids > PAHs >

TABLE 5. Weighting Factors, ^{i}b (27)

compound	^{i}b
all alkanes of carbon no. 16−22	0.09 (0.07−0.13)
PAHs	0.13
9,10-anthraquinone	0.14
aromatic carboxaldehyde	0.12
alkanoic acid	0.12
substituted phenols (nonhindered)	0.25
9-phenanthrol	0.2
9-nitroanthracene	0.13
$D_4D'OH$	0.07

alkanes. For diesel soot, activity coefficients of ~1 were estimated for alkanes by both methods. This would be expected since diesel soot particles have a high content of long-chain alkanes and alkanoic acids. For diesel soot, UNIFAC tended to be a bit higher than the Hansen method for PAHs, and was a factor of 4 higher for PAH carboxaldehydes. For α-pinene/O_3 aerosols, UNIFAC and the Hansen method gave similar $^{i}\gamma_{om}$ values for PAHs. Although both methods correctly gave high activity coefficients for alkanes on these particles, UNIFAC was a factor of 5−7 higher than Hansen. The differences in the computational approaches are responsible for predicted activity coefficient differences.

Theory vs Chamber Data. To generate semivolatile G/P partitioning data for model comparisons, separate chamber experiments were conducted with wood smoke particles, diesel combustion particles, and secondary aerosols from the reaction of α-pinene and O_3. Compounds shown in Table 7 were monitored. G/P data were used to calculate the experimental partitioning coefficients, K_p, according to $K_p = (F/\mathrm{TSP})/A$ (eq 1). Log K_p for each compound was then plotted vs log p_L^o calculated at the temperature observed during sampling. Vapor pressures were calculated using different literature techniques: PAHs, Yamasaki *et al. (39)*; alkanes, interpolated from Pankow *et al. (6, 40)*; alkanoic acids, Tao *et al.* (41); 1-hydroxynonamethylcyclopentasiloxane ($D_4D'OH$), Dow Corning *(42)*; other compounds, Reid *et al. (43)*. For some compounds it was necessary to estimate boiling points according to Joback's method, as described by Jones and Bursey *(44)*, which were used to calculate entropies of vaporization and vapor pressures *(12)*. Different vapor pressure calculation techniques *(12, 39, 40, 43, 44)* generally agree to within a factor of 2 or 3 (0.3−0.5 on a log scale), but larger differences are possible.

Given the range of errors associated with gas and particle sampling, a maximum standard deviation of ±25% for K_p was estimated. In spite of vapor pressure and K_p errors, the importance of activity coefficients, $^{i}\gamma_{om}$, in predicting the G/P partitioning can still be successfully demonstrated over a wide range of vapor pressures (10^{-2} to 10^{-7} torr) for many different types of SOCs. Figure 1A shows the experimental log K_p values for SOCs on wood smoke particles at a temperature of 22 °C and a relative humidity of 88%. When log K_p was plotted vs log p_L^o, a regression line with some scatter was obtained (slope = 0.80 and $r^2 = 0.66$). However, the inclusion of $^{i}\gamma_{om}$, as calculated from the UNIFAC model (to give $K_{p,\gamma}$ as per eq 3), dramatically improved the relationship. A plot of log $K_{p,\gamma}$ vs log p_L^o had a slope of 1.07 and an r^2 of 0.92 (Figure 1B). UNIFAC interaction parameters were unavailable for siloxanes, 9,10-anthraquinone, and 9-nitroanthracene, so the Hansen's group contribution method was used for these compounds. With wood smoke, when the Hansen technique was used to estimate all of the $^{i}\gamma_{om}$ values, similar improvements to the partitioning fits were obtained. In Figure 1B, BHT (2,6-di-*tert*-butyl-4-methylphenol) was excluded from the regression analysis, because the activity coefficient of BHT may be underestimated by UNIFAC. This is because UNIFAC cannot account for geometric effects as well as specific strong interactions such as a hydrogen bonding. For example, the phenolic group of BHT is hindered by tertiary butyl groups in the 2 and 6 positions. Hence, it was not surprising that the BHT point was outside of the 90% confidence interval for the estimated $^{i}K_{p,\gamma}$ values in wood soot, which is dominated by substituted phenols and aromatic carboxylic acids.

Partitioning of SOCs onto secondary aerosols formed from the α-pinene/O_3 reaction is shown in Figure 2. An experimental slope of −0.53 was obtained from a log K_p vs log p_L^o correlation (Figure 2A, $r^2 = 0.31$). This improved to a slope of −0.94 (Figure 2B, $r^2 = 0.84$) when log $K_{p,\gamma}$ was plotted vs log p_L^o using activity coefficients from UNIFAC. Although

TABLE 6. Comparison of Activity Coefficients of Organic Compounds Using UNIFAC and Hansen Group Contribution Methods at RH = 0%

compound	UNIFAC wood[a]	Hansen wood[a]	UNIFAC diesel[b]	Hansen diesel[b]	UNIFAC α-pinene/O_3[a]	Hansen α-pinene/O_3[a]
anthracene	2.8	3.4	2.8	1.7	3.6	2.4
phenanthrene	2.8	3.9	2.8	1.3	3.6	2.5
pyrene	4.0	4.0	4.3	2.6	5.3	2.7
fluoranthene	4.0	3.9	4.3	2.2	5.3	2.6
benz[a]anthracene	4.1	5.6	4.8	5.2	5.7	3.8
9-methylanthracene	2.1	3.9	2.9	1.8	4.2	2.6
heptadecane	27.3	28.1	1.2	1.2	38.8	10.6
nonadecane	36.4	33.8	1.2	1.2	54.3	11.6
eicosane	41.9	37.0	1.2	1.2	63.9	12.1
docosane	55.1	44.2	1.2	1.2	88.2	13.2
dodecanoic acid	2.8	3.0	1.5	1.1	2.1	2.1
tetradecanoic acid	3.5	3.4	1.4	1.1	2.7	2.3
hexadecanoic acid	4.4	5.3	mc[c]	1.1	3.5	3.0
9,10-anthraquinone	na[c]	2.5	na	5.7	na	1.9
9-nitroanthracene	na	2.7	na	4.0	na	1.8
phenanthrene-9-carboxaldehyde	1.8	1.8	11.5	2.9	3.3	1.5
4-biphenylcarboxaldehyde	1.5	1.6	8.4	2.3	2.5	1.4
BHT	0.9	1.4	1.6	2.7	0.6	1.3
vanillin	2.5	2.9	198.0	98.8	cnp[c]	4.1
3,5-dimethylphenol	0.8	1.2	2.4	2.5	0.4	1.4
2-isopropylphenol	0.9	1.1	2.0	2.8	0.3	1.3
decamethylcyclopentasiloxane (D_5)	na	64.9	na	1.7	na	22.6
$D_4D'OH$	na	24.6	na	2.1	na	12.2

[a] At 295 K. [b] At 285 K. [c] na: UNIFAC interaction parameters were not available. mc: was used as a major aerosol component (see Table 3). cnp: calculation not possible because there were too many functional groups for calculation.

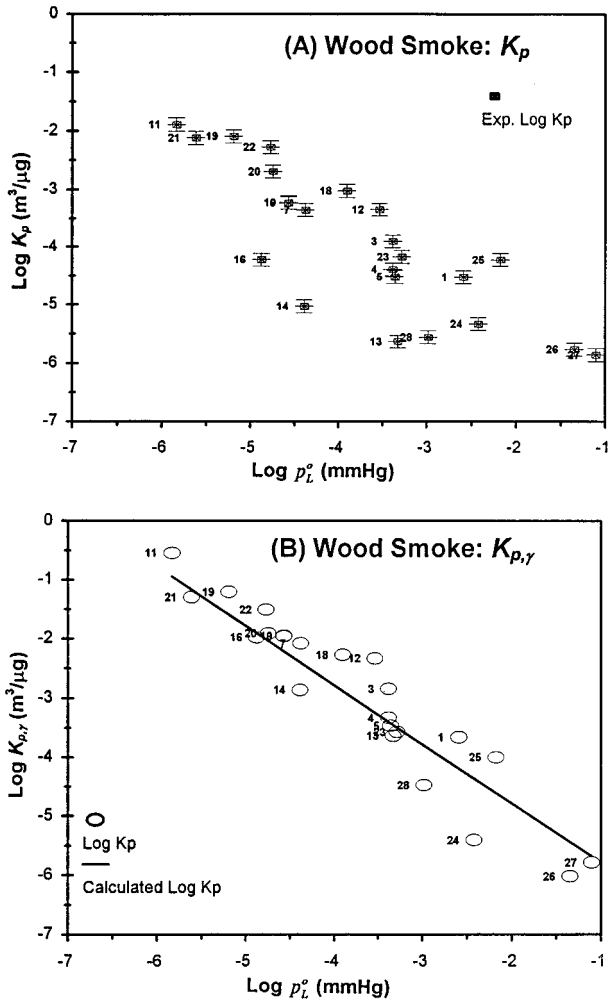

FIGURE 1. (A) Log K_p values vs log p_L^o correlation for semivolatile compounds on wood smoke particles (Aug. 14, 1996) with 1 standard deviation error bands for log K_p values. The temperature was 22 °C, and the RH was 88%. Numbers correspond to compounds listed in Table 7. (B) Log $K_{p,\gamma}$ values vs log p_L^o for semivolatile compounds on the same wood smoke particles as Figure 1A. The solid line is a idealized plot of log $K_{p,\gamma}$ vs log p_L^o for wood soot, with $f_{om} = 0.85$ and $MW_{om} = 94.3$.

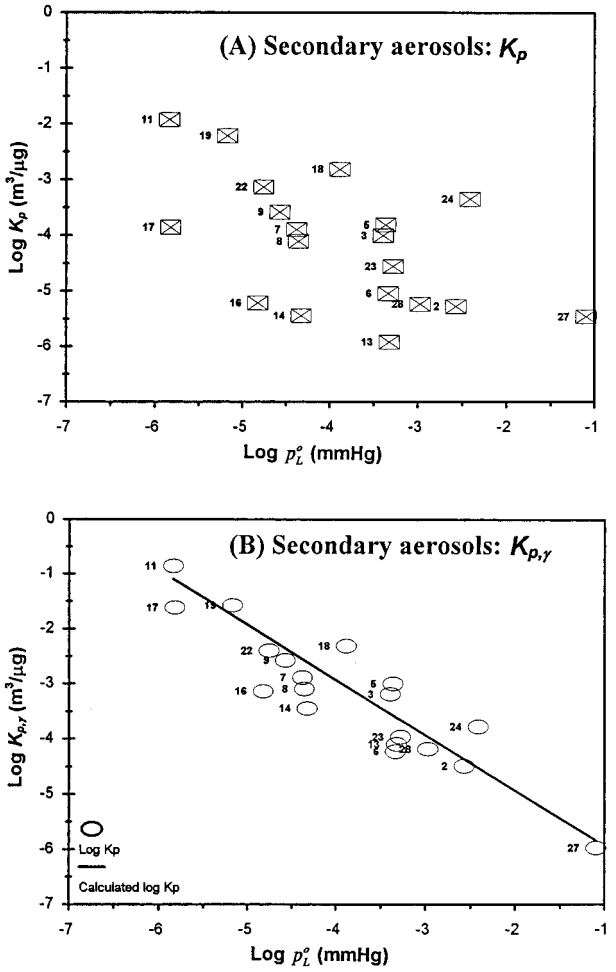

FIGURE 2. (A) Log K_p vs log p_L^o for semivolatile compounds partitioning on to an α-pinene/ozone aerosol (Aug. 5, 1996) at 23 °C and 58% RH. Numbers correspond to compounds listed in Table 7. (B) Log $K_{p,\gamma}$ values vs log p_L^o for semivolatile compounds on the same α-pinene/ozone aerosol in Figure 2A. The solid line is an idealized plot of log $K_{p,\gamma}$ vs log p_L^o.

these results give approximately the desired theoretical slope of near −1 (eq 4), we did not see a systematic reason why some compounds deviated more than others from the ideal partitioning line in Figure 2. When the Hansen method was used with secondary aerosols to calculate all the activity coefficients, more scatter was observed in log $K_{p,\gamma}$ vs log p_L^o regressions than when UNIFAC was used.

As a final example in this study, two outdoor chamber experiments were simultaneously conducted on the same day. Wood smoke particles were added to one chamber and diesel soot to the other. Gas and particle samples were taken from both chambers within 30 min of each other, and hence sampling from the two chambers occured under similar temperature and humidity conditions (Table 1). In eq 4, both wood and diesel soot would have different intercepts, log $[f_{om}(7.501RT)/(10^9 MW_{om})]$, because the values of f_{om} and MW_{om} are different in the different media. Since f_{om} and MW_{om} were estimated for both diesel and wood soot particles, the quantity log $[f_{om}(7.501RT)/(10^9 MW_{om})]$ can be subtracted from the log $K_{p,\gamma}$ values for each compound. This permits SOCs from both the diesel and wood soot experiments to be plotted on the same log $K_{p,\gamma}$ vs log p_L^o graph. As shown in Figure 3 (UNIFAC model), a good fit was observed for partitioning data derived from these two very different particle systems (slope = −1.07, $r^2 = 0.96$).

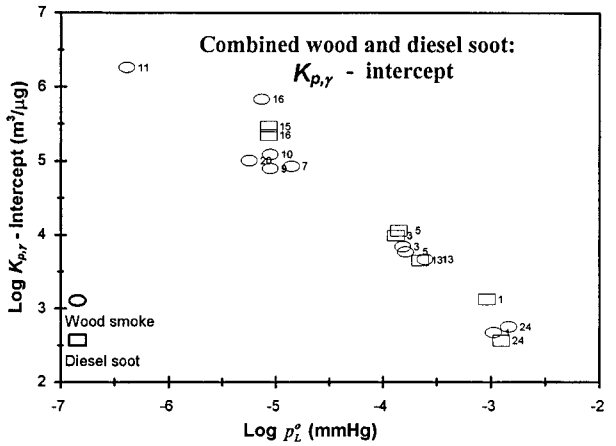

FIGURE 3. Intercept-adjusted log $K_{p,\gamma}$ values vs log p_L^o for semivolatile compounds from separate diesel and wood soot experiments on the same day (October 25, 1995).

These results suggest that activity coefficients can vastly improve our ability to calculate the partitioning of a variety of different SOCs having a range of polarities. For conditions when the atmosphere is close to equilibrium, this approach can be applied directly. When the atmosphere is not in equilibrium, these predictions of equilibrium become the chemical potential "driver" for intraparticle diffusion models of the type developed by our lab and by others (*46*−*48*). As

TABLE 7. Vapor pressures for compounds at 295K and 285K (mmHg)

no.	compounds	log p_L^o at 295 K	log p_L^o at 285 K	ref
1	fluorene	−2.63	−3.06	39
2	d_{10}-fluorene[a]	−2.62	−3.05	39
3	anthracene	−3.43	−3.91	39
4	d_{10}-anthracene[a]	−3.43	−3.90	39
5	phenanthrene	−3.42	−3.88	39
6	d_{10}-phenanthrene[a]	−3.39	−3.86	39
7	fluoranthene	−4.44	−4.96	39
8	d_{10}-fluoranthene[a]	−4.42	−4.95	39
9	pyrene	−4.64	−5.16	39
10	d_{10}-pyrene[a]	−4.62	−5.16	39
11	benz[a]anthracene	−5.91	−6.51	39
12	9-methylanthracene	−3.59	−4.08	12,43
13	d_{36}-heptadecane[b]	−3.36	−3.67	6,40
14	d_{38}-nonadecane[b]	−4.40	−4.55	6,40
15	eicosane	−4.89	−5.08	6,40
16	d_{42}-eicosane[b]	−4.89	−5.08	6,40
17	docosane	−5.84	−6.31	6,40
18	myristic acid	−4.01	−5.03	41
19	palmitic acid	−5.31	−6.41	41
20	9,10-anthraquinone	−4.80	−5.36	12,43
21	9-nitroanthracene	−5.67	−6.26	12,43
22	phenanthrene-9-carboxaldehyde	−4.83	−5.38	12,43
23	4-biphenylcarboxaldehyde	−3.33	−3.82	12,43
24	BHT	−2.47	−2.94	12,43
25	vanillin	−2.22	−2.65	12,43
26	3,5-dimethylphenol	−1.39	−1.80	12,43
27	2-isopropylphenol	−1.15	−1.55	12,43
28	$D_4D'OH$	−3.05	−3.72	42

[a] The vapor pressures of deuterated PAHs were based on nondeuterated PAH liquid vapor pressured data from Yamasaki and Kuge *(39)*. [b] The vapor pressures of deuterated alkanes were based on nondeuterated alkanes *(6,40)*.

such, this work is an additional step in developing the ability to predict the partitioning and ultimately the fate of SOCs in the atmosphere under various conditions.

Acknowledgments

This work was supported by a grant from the National Science Foundation to the University of North Carolina (ATM 940848, Dr. Sherry O. Farewell project officer) and a gift from Dow Corning under the direction of Dr. Grish Chandra.

Literature Cited

(1) Bidleman, T. F.; Billings, W. N.; Foreman, W. T. *Environ. Sci. Technol.* **1986**, *20*, 1038−1043.
(2) Pankow, J. F. *Atmos. Environ.* **1987**, *21*, 2275−2283.
(3) Pankow, J. F. *Atmos. Environ.* **1991**, *25A*, 2229−2239.
(4) Pankow, J. F.; Bidleman T. F. *Atmos. Environ.* **1992**, *26A*, 1071−1080.
(5) Pankow, J. F. *Atmos. Environ.* **1994**, *28*, 185−188.
(6) Pankow, J. F.; Isabelle, L. M.; Bucholz, D. A.; Luo, W.; Reeves, B. D. *Environ. Sci. Technol.* **1994**, *28*, 363−365.
(7) Kamens, R. M.; Odum, J.; Fan, Z. *Environ. Sci. Technol.* **1995**, *29*, 43−50.
(8) McDow, S. R.; Jang, M.; Hong, Y.; Kamens, R. M. *J. Geophys. Res.* **1996**, *101*, 19593−19600.
(9) Kamens, R. M.; Guo, Z.; Fulcher, J. N.; Bell, D. A. *Environ. Sci. Technol.* **1988**, *22*, 103−108.
(10) Fan, Z.; Kamens, R. M.; Hu, J.; Zhang, J. *Environ. Sci. Technol.* **1996**, *30*, 1359−1364.
(11) Gundel, L. A.; Lee, V. C.; Mahanama, K. R. R.; Stevens, R. K.; Daisey, J. M. *Atmos. Environ.* **1995**, *29*, 1719−1733.
(12) Schwarzenbach, R. P.; Gschwend, P. M.; Imboden, D. M. *Environmental Organic Chemistry*; John Wiley & Sons Inc.: New York, 1993.
(13) Barton, A. F. M. *Handbook of Solubility Parameters and Other Cohesion Parameters*, 2nd ed.; CRC Press: Boston, 1991.
(14) Sandler, S. I. *Chemical and Engineering Thermodynamics*; John Wiley & Sons Inc.: New York, 1989.
(15) Meusburger, K. E. *Am. Chem. Soc. Symp. Ser.* **1988**, *371*, 151−162.
(16) Chen, F.; Holten-Anderson, J.; Tyle, H. *Chemosphere* **1993**, *26*, 1325−1354.
(17) Kan, A. T.; Tomson, M. B. *Environ. Sci. Technol.* **1996**, *30*, 1369−1376.
(18) Arbuckle, W. B. *Environ. Sci. Technol.* **1983**, *17*, 537−542.
(19) Nielsen, F.; Olsen, E.; Fredenslund, A. *Environ. Sci. Technol.* **1994**, *28*, 2133−2138.
(20) Hildebrand, J. H.; Scott, R. L. *Solubility of Non-Electrolytes*, 3rd ed.; Reinhold Publishing Cor.: New York, 1950.
(21) Hildebrand, J. H.; Scott, R. L. *Regular Solutions*; Prentice-Hall Inc.: Englewood Cliffs, NJ, 1962.
(22) Barton, A. F. M. *Chem. Rev.* **1975,** *75*, 731−753.
(23) Hansen C. M. *J. Paint Technol.* **1969**, *39*, 104−117.
(24) Van Krevlen, D. W. *Properties of Polymers: Their Correlation with Chemical Structure; Their Numerical Estimation and Prediction from Additive Group Contributions*, 3rd ed.; Elsevier Science Publisher: New York, 1990.
(25) Bicerano, J. *Prediction of Polymer Properties*; Marcel Dekker Inc.: New York, 1993.
(26) Hansen, C. M.; Andersen, B. H. *Am. Ind. Hyg. Assoc. J.* **1988**, *49*, 301−308.
(27) Lo, T. C.; Baird, M. H. I.; Hanson, C. *Handbook of Solvent Extraction*; John Wiley & Sons. Inc.: New York, 1983.
(28) Fredenslund, A.; Sorensen, J. M. Group Contribution Estimation Methods. *Models for Thermodynamic and Phase Equilibria Calculations*; Heinemann, H., Ed.; Marcel Dekker Inc.: New York, 1994.
(29) Gmehling, J.; Rasmussen, P.; Fredenslung, A. *Ind. Eng. Chem. Res.* **1982**, *21*, 118−127.
(30) Hansen, H. K.; Rasmussen, P. *Ind. Eng. Chem. Res.* **1991**, *30*, 2352−2356.
(31) Fredenslung, A.; Jones, R. M.; Prausnitz, J. M. *AIChE J.* **1975**, *21*, 1086.
(32) Hawthorne, S. B.; Krieger, M. S.; Miller, D. J.; Mathiason, M. B. *Environ. Sci. Technol.* **1989**, *22*, 470−475.
(33) Jang, M.; McDow, S. R. *Environ. Sci. Technol.* **1995**, *29*, 2654−2660.
(34) McDow, S. R.; Sun, Q.; Vartiainen, M.; Hong, Y.; Yao, Y.; Fister, T.; Yao, R. Q.; Kamens, R. M. *Environ. Sci. Technol.* **1994**, *28*, 2147−2153.
(35) Odum, J.; McDow, S. R.; Kamens, R. M. *Environ. Sci. Technol.* **1994**, *28*, 1285−1290.
(36) Rogge, W. F.; Hildemann, L. M.; Mazurek, M. A.; Cass, G. R. *Environ. Sci. Technol.* **1993**, *27*, 636−651.
(37) Rogge, W. F. Pine, Oke, and Synthetic Log Combustion in Residential Fireplaces. *Determination of Key Organic Compounds Present in the Particulate Matter Emissions from Air Pollution Sources*; final report to EPA, Contract No. 8932-127, CA., 1993.
(38) Hull, L. A., Terpene ozonolysis products. In *Atmospheric Biogenic Hydrocarbons*; Bufalini, J. J., Arnts, R. R., Eds.; Ann Arbor Science Publishers Inc., 1981; vol 2, pp 161−186.
(39) Yamasaki, H. K.; Kuge, Y. *Nippon Kagaku Kaishi* **1984**, *8*, 1324−1329.
(40) Story, J. M.; Lou, W.; Isabelle, L. M.; Pankow, J. F. *Environ. Sci. Technol.* **1995**, *29*, 1519−1523.
(41) Tao, Y.; McMurry, P. H. *Environ. Sci. Technol.* **1989**, *23*, 1519−1523.
(42) Grish, G.; Experimental data on the vapor pressure of D4D'OH provided by the Dow Corning Corporation of Midland Michigan, 1995.
(43) Reid, R. C.; Prausnitz, J. M.; Poling, B. E. *The Properties of Gases and Liquids*, 4th ed.; McGraw-Hill Co.: New York, 1987.
(44) Jones, D. L.; Bursey, J. Simultaneous Control of PM-10 and Hazard Air Pollutants Final Report to USEPA; Gary S. Blais EPA/452-R-93-013, RTP NC, 27711.
(45) Staudinger, J.; Roberts, P. V. *Crit. Rev. Environ. Sci. Technol.* **1996**, *26(3)*, 205−297.
(46) Odum, J.; McDow, S. R.; Kamens, R. M. *Environ. Sci. Technol.* **1994,** *28*, 1285−1290.
(47) Rounds, S. A.; Tiffany, B. A.; Pankow, J. F. *Environ. Sci. Technol.* **1993,** *27*, 366−377.
(48) Strommen, M. R.; Kamens, R. M. *Environ. Sci. Technol.* **1997**, *31*, 2983−2990.

Received for review January 6, 1997. Revised manuscript received June 19, 1997. Accepted June 20, 1997.[⊗]

ES970014D

[⊗] Abstract published in *Advance ACS Abstracts*, August 15, 1997.